

# Solvent-Driven Conformational Exchange for Amide-Linked Bichromophoric BODIPY Derivatives

Shrikant Thakare,<sup>[a]</sup> Patrycja Stachelek,<sup>[b]</sup> Soumyaditya Mula,<sup>[c]</sup> Ankush B. More,<sup>[a]</sup> Subrata Chattopadhyay,<sup>[c]</sup> Alok K. Ray,<sup>[d]</sup> Nagaiyan Sekar,<sup>[a]</sup> Raymond Ziessel<sup>[e]</sup> and Anthony Harriman<sup>[b],\*</sup>

**Abstract:** The fluorescence lifetime and quantum yield are seen to depend in an unexpected manner on the nature of the solvent for a pair of tripartite molecules comprising two identical boron dipyrromethene (BODIPY) residues attached to a 1,10-phenanthroline core. A key feature of these molecular architectures concerns the presence of an amide linkage that connects the BODIPY dye to the heterocyclic platform. The secondary amide derivative is more sensitive to environmental change than is the corresponding tertiary amide. In general, increasing solvent polarity, as measured by the static dielectric constant, above a critical threshold tends to reduce fluorescence but certain hydrogen bond accepting solvents exhibit anomalous behavior. Fluorescence quenching is believed to arise from light-induced charge transfer between the two BODIPY dyes but thermodynamic arguments alone do not explain the experimental findings. Molecular modelling is used to argue that the conformation changes in strongly polar media in such a way as to facilitate improved rates of light-induced charge transfer. These solvent-induced changes, however, differ remarkably for the two types of amide.

## Introduction

The amide bond plays a special role in biochemistry whereby it provides the key structural features needed to assemble helical peptides and folded proteins.<sup>[1,2]</sup> Indeed, the amide carbonyl function is less electrophilic than in ketones, aldehydes and carboxylic acids while  $sp^2$  hybridisation renders the nitrogen atom non-basic.<sup>[3]</sup> This latter point is well illustrated by the fact that protonation of amides in acidic media occurs at the oxygen atom. In general, the amide group persists in two tautomeric forms; namely, the amide and iminol structures.<sup>[4]</sup> However, the amide

form is generally considered as a set of zwitterionic resonance structures (Chart 1). In each case, both *trans*- and *cis*-forms are possible. The partial double-bond character imposed on the central C-N bond helps position the atoms around the amide bond such that they reside in the same plane and provides a high (i.e., 10-25 kcal/mol) barrier for internal rotation.<sup>[4d]</sup> In most proteins, the amide-*trans* tautomer (Chart 1) is the more stable species but the corresponding amide-*cis* form has been clearly recognized by X-ray crystallography. Indeed, the amide-*cis* tautomer is often found in simple amides, such as formamide and N-methylacetamide.<sup>[5]</sup> Much less information is available regarding the possible occurrence of amide-iminol tautomerism for the amide bond (Chart 1), although this situation is interesting from the theoretical viewpoint.<sup>[6]</sup> Such transformations, which require a large structural rearrangement, might be more easily accomplished in solution, especially in the presence of hydrogen-bonding solvents. It is also significant that the amide oxygen atom is a good hydrogen-bond acceptor while the nitrogen atom is an effective hydrogen-bond donor. This aspect of amide chemistry is of crucial importance in terms of establishing the secondary structures of proteins, enzymes, bacteria, viruses, *etc.* and has been studied in great detail.<sup>[7]</sup>

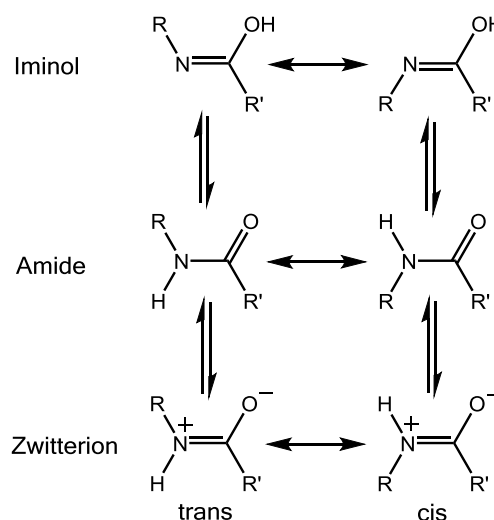


**Chart 1.** Major tautomeric and resonance forms of the amide bond; the positive charge assigned to the nitrogen atom should not be taken literally since the overall electronic charge at this site is likely to remain negative.

[a] S. Thakare, A. B. More, Prof. N. Sekar  
Department of Dyestuff Technology, Institute of Chemical  
Technology, Mumbai-400019, India

[b] P. Stachelek, Prof. Dr. A. Harriman  
Molecular Photonics Laboratory, School of Chemistry, Bedson  
Building, Newcastle University, Newcastle upon Tyne, NE1 7RU,  
United Kingdom  
E-mail: anthony.harriman@ncl.ac.uk

[c] Dr. S. Mula, Prof. S. Chattopadhyay  
Bio-Organic Division, Bhabha Atomic Research Centre, Mumbai-  
400085, India  
E-mail: smula46@gmail.com

[d] Prof. A. K. Ray  
Laser and Plasma Technology Division, Bhabha Atomic Research  
Centre, Mumbai-400085, India

[e] Dr. R. Ziessel,  
Laboratoire de Chimie Organique et Spectroscopies Avancées  
(LCOSA), Ecole Européenne de Chimie, Polymères et Matériaux,  
Université de Strasbourg, 25 rue Becquerel, 67087 Strasbourg  
Cedex 02, France.

The amide bond, although relatively small, might be expected to help dictate the global structures of large organic molecules and even supramolecular entities.<sup>[8]</sup> This realization takes on additional importance when allowance is made for the fact that the amide linkage can be sensitive to changes in the local environment. We now report bichromophoric molecules, BAB(H) and BAB(ET), wherein two identical boron dipyrromethene (BODIPY) dyes are appended at the 2,9-positions of a 1,10-phenanthroline residue by way of amide connectors (Figure 1). Such BODIPY dyes are highly fluorescent markers<sup>[9]</sup> that, at least in the case of monomeric dyes, are insensitive to the nature of the surrounding medium, temperature or pressure.<sup>[10]</sup> The specific intention of this work is to explore whether the amide bond, which constitutes less than 3% of the total solvent-accessible surface area of the supermolecule, can exert control over the molecular geometry. It might be noted that there is a complete library of BODIPY derivatives bearing aryl hydrocarbons attached directly to the dipyrin backbone or through the pseudo-*meso*-position<sup>[9]</sup> but none of these structures use an amide spacer as the means by which to interconnect the terminals.

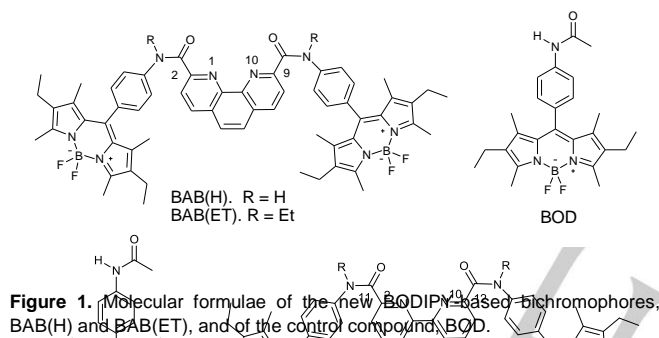
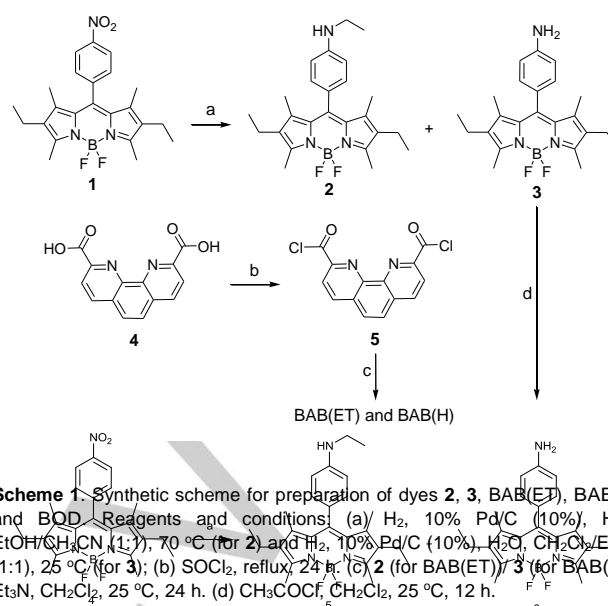


**Figure 1.** Molecular formulae of the new BODIPY-based bichromophores, BAB(H) and BAB(ET), and of the control compound, BOD.

Our strategy is based on the realization that the BODIPY dyes are likely to be strongly fluorescent when embedded in a solvent reservoir.<sup>[11]</sup> Rotations around the connecting units should ensure that the two BODIPY dyes remain mutually independent and it might be noted that NMR spectra are fully consistent with this notion. In the event that the amide connector responds to changes in the nature of the surrounding solvent, the molecular conformation might be expected to change in such a way that the two BODIPY fluorophores are brought into closer proximity. In turn, this effect should be visualized by a change in the overall fluorescence output. The idea behind using 1,10-phenanthroline is to make use of its well-known ability<sup>[12]</sup> to complex cations from solution, including protons. It is also apparent that repulsion between lone-pairs on the carbonyl and aza-nitrogen atoms should help establish the molecular conformation. If successful, this approach could be adapted to generate related structural changes brought about by external or internal triggering so that the kinetics for the folding and/or unfolding steps might be monitored. Such information could be helpful in terms of better understanding the critical issues of protein denaturation<sup>[13]</sup> and unfolding.<sup>[14]</sup>



**Scheme 1.** Synthetic scheme for preparation of dyes 2, 3, BAB(ET), BAB(H) and BOD. Reagents and conditions: (a) H<sub>2</sub>, 10% Pd/C (10%), H<sub>2</sub>O, EtOH/CH<sub>3</sub>CN (1:1), 70 °C (for 2) and H<sub>2</sub>, 10% Pd/C (10%), H<sub>2</sub>O, CH<sub>2</sub>Cl<sub>2</sub>/EtOH (1:1), 25 °C (for 3); (b) SOCl<sub>2</sub>, reflux, 24 h; (c) 2 (for BAB(ET)), 3 (for BAB(H)), Et<sub>3</sub>N, CH<sub>2</sub>Cl<sub>2</sub>, 25 °C, 24 h. (d) CH<sub>3</sub>COCl, CH<sub>2</sub>Cl<sub>2</sub>, 25 °C, 12 h.

## Results and Discussion

### Synthesis and Characterization

Synthesis of the target bichromophoric molecules BAB(ET) and BAB(H), which differ only in terms of the substitution pattern at the amide sites, was aided by earlier work<sup>[15]</sup> which explored the catalytic hydrogenation of the corresponding mononuclear BODIPY derivative, 1, bearing a *meso*-4-nitrophenyl group. Thus, the Pd-catalyzed hydrogenation of 1 in a mixture of dichloromethane and ethanol at 25 °C gave the expected amino-BODIPY 3 as the only product. However, when the reaction was carried out in a mixture of acetonitrile and ethanol at 70 °C, dye 2 was the major product along with a small amount of 3 (2:3 = 95:5) (Scheme 1). Apparently, the initially formed 3 is readily transformed to 2 by an *in situ* reaction with CH<sub>3</sub>CN.<sup>[16]</sup> Compound 3 was acetylated with acetyl chloride in CH<sub>2</sub>Cl<sub>2</sub> to obtain the control compound, BOD, in 81% yield (Figure 1 and Scheme 1). The target compounds BAB(ET) and BAB(H) were synthesized by reacting 1,10-phenanthroline-2,9-diacid chloride<sup>[17]</sup> with 2 and 3, respectively. After workup and purification by flash chromatography, the desired compounds were isolated in 42% and 52% yield, respectively (Scheme 1).

The target compounds were characterized fully by NMR spectroscopy, giving well-defined spectra. For example, in the case of dye BAB(H), aromatic protons of the 1,10-phenanthroline unit appear as two different sets of signals. Protons of the central aromatic ring resonate as a singlet at 8.04 ppm whereas the other aromatic protons exhibit two doublets at 8.57 and 8.74 ppm. The methyl groups of the BODIPY moieties resonate as singlets at 1.35 and 2.50 ppm, while the ethyl groups resonate as quartets (2.22 ppm) and triplets (0.91 ppm). The aromatic phenyl protons of the two BODIPY units are found as doublets at 7.33 and 8.11

## FULL PAPER

ppm with the expected 4-proton integration for each signal. A diagnostic signal is provided by the N-H proton which is found as a singlet at 10.88 ppm. The carbon-13 NMR spectra present the expected 4 and 15 signals for the alkyl and aromatic carbon atoms, respectively. The amide carbonyl signal is found at 162.1 ppm in  $\text{CDCl}_3$ .

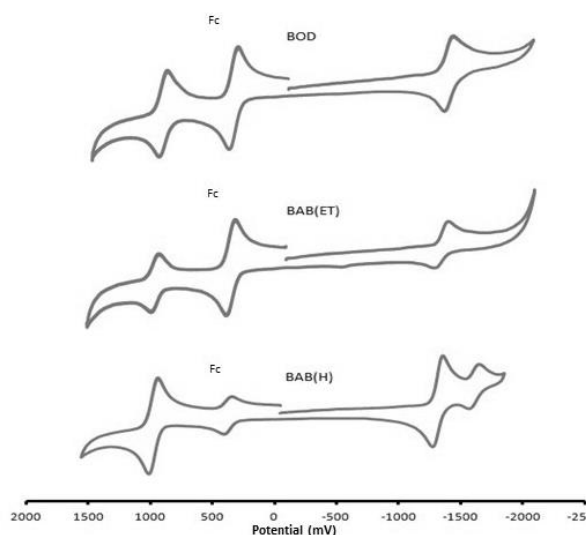


**Figure 2.** Typical cyclic voltammograms recorded for the target compounds (ca. 2 mM) in de-aerated  $\text{CH}_2\text{Cl}_2$  containing background electrolyte. Note Fc refers to ferrocene used as internal standard. The lower axis corresponds to mV vs SCE.

## Electrochemistry

Cyclic voltammetry studies were carried out for the target compounds, BOD, BAB(ET) and BAB(H), in both  $\text{CH}_2\text{Cl}_2$  and  $\text{CH}_3\text{CN}$  with tetra-*N*-butylammonium hexafluorophosphate as the supporting electrolyte and the main results are summarized by way of Table 1. The control compound, BOD, exhibits *quasi*-reversible one-electron oxidation and reduction steps with half-wave potentials of +0.95 V and -1.40 V vs SCE, respectively, that can be assigned to formation of the corresponding  $\pi$ -radical cation and anion (Figure 2).<sup>[18]</sup> The amide function has no effect on the reduction potentials and does not make a direct contribution to the cyclic voltammograms. The two solvents give comparable results. For BAB(ET), similar oxidation and reduction processes are observed, with much the same half-wave potentials to those noted for the control compound, and there are no undue effects associated with the bridging 1,10-phenanthroline unit. With the bichromophore, however, both processes involve the *quasi*-reversible transfer of two electrons. That the two electrons are transferred at the same potential is taken as testimony to the fact that the BODIPY units do not interact in an electronic sense.

Although BAB(H) displays similar behavior to that noted for BAB(ET), there is indication for the one-electron reduction of the

1,10-phenanthroline-based bridge at about -1.6 V vs SCE (Figure 2). The appearance of this wave is attributed to internal hydrogen bonding between the aza-N atom and the amide proton. In fact, this situation was confirmed by infra-red spectroscopy. The significance of these results is that light-induced charge transfer between the BODIPY units and the bridging 1,10-phenanthroline unit is thermodynamically unfavorable, even in polar solvent. The electrochemistry also indicates that there is no electronic interaction between the appended BODIPY residues.

**Table 1.** Electrochemical data recorded for the target BODIPY-based dyes in  $\text{CH}_2\text{Cl}_2$ .<sup>[a]</sup>

| Compound | $E_{\text{ox}}^0$ , V ( $\Delta E$ , mV) | $E_{\text{red}}^0$ , V ( $\Delta E$ , mV) |
|----------|--|---|
| BOD      | +0.57 (32)                               | -1.77 (74)                                |
| BAB(ET)  | +0.61 (66)                               | -1.69 (70)                                |
| BAB(H)   | +0.60 (82)                               | -1.69 (62); -1.98 (78)                    |

[a] Half-wave potentials determined by cyclic voltammetry in deoxygenated  $\text{CH}_2\text{Cl}_2$  solution, containing 0.1M TBAPF<sub>6</sub>, at a solute concentration of 1.5 mM at 25 °C. Potentials were standardized using ferrocene (Fc) as an internal reference and the half-wave potentials are reported relative to the Fc/Fc<sup>+</sup> couple. Error in half-wave potentials is  $\pm 15$  mV.

**Table 2.** Comparison of the photophysical properties determined for the target compounds in THF solution at room temperature.

| Compound | $\lambda_{\text{MAX}}$ / nm | $\lambda_{\text{FLU}}$ / nm | $\Phi_{\text{F}}$ | $\tau_{\text{S}}$ / ns | SS / $\text{cm}^{-1}$ [a] | $k_{\text{RAD}} / 10^8 \text{ s}^{-1}$ [b] |
|----------|-----------------------------|-----------------------------|-------------------|------------------------|---------------------------|--|
| BOD      | 523                         | 536                         | 0.80              | 5.9                    | 465                       | 1.38                                       |
| BAB(H)   | 522                         | 540                         | 0.73              | 5.4                    | 640                       | 1.40                                       |
| BAB(ET)  | 524                         | 538                         | 0.75              | 5.5                    | 500                       | 1.40                                       |

[a] SS refers to the Stokes' shift for normalized spectra. [b] Radiative rate constant calculated from the Strickler-Berg expression.

## Photophysical Properties

The absorption and fluorescence spectra recorded for the control compound, BOD, in tetrahydrofuran (THF) at room temperature are entirely in accord with what might be expected for a conventional BODIPY dye.<sup>[9]</sup> The absorption maximum ( $\lambda_{\text{MAX}}$ ) lies at 523 nm while the emission maximum ( $\lambda_{\text{FLU}}$ ) is found at 536 nm. Both values are unremarkable when considered in terms of related BODIPY derivatives.<sup>[19]</sup> Moreover, both the fluorescence quantum yield ( $\Phi_{\text{F}} = 0.80$ ) and excited-singlet state lifetime ( $\tau_{\text{S}} = 5.9$  ns) are in line with values recorded for structurally related dyes.<sup>[9,19]</sup> There is excellent agreement between absorption and excitation spectra and the time-resolved emission decay profiles are well described by mono-exponential fits. Changes in solvent polarity have little effect on these various parameters, although the absorption and emission maxima do respond slightly to changes in solvent polarizability.<sup>[20]</sup> Spectral properties recorded for the bichromophores under identical conditions are closely

comparable to those recorded for BOD (Table 2, Figure 3). Thus, we can conclude that there are no undue electronic effects associated with either the amide linker or the 1,10-phenanthroline spacer. In THF solution, the quantum yields and excited-state lifetimes recorded for BAB(ET) and BAB(H) are comparable to those found for BOD, although fluorescence is decreased slightly, especially for BAB(H) (Table 2). For the two bichromophores, excitation and absorption spectra are in close agreement and time-resolved decay curves remain mono-exponential over at least three half-lives. The presence of molecular oxygen does not affect the derived properties while changes in solvent polarity have only minimal effect on the absorption and emission spectral maxima and on the band half-widths.

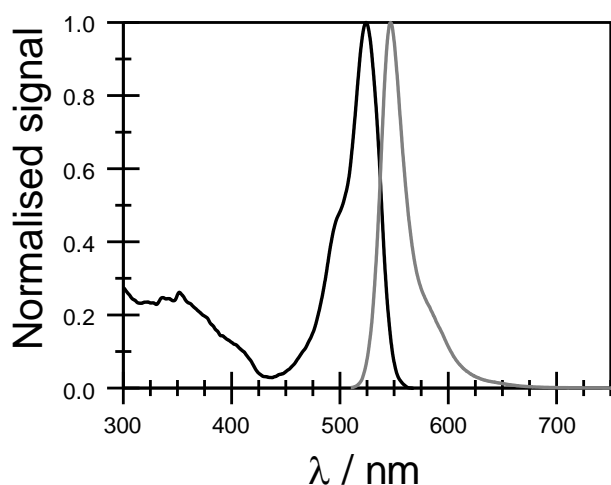


**Figure 3.** Normalized absorption (black curve) and fluorescence (grey curve) spectra recorded for BAB(H) in THF solution at room temperature.

The photophysical properties of the tertiary amide derivative, BAB(ET), were recorded in a range of organic solvents of differing dielectric constant,  $\epsilon_S$ , and the results are summarized in Table 3. The variation in  $\Phi_F$  is small across the range of solvents, despite  $\epsilon_S$  changing from 2 to 47 and there is no noticeable influence of hydrogen-bond donor solvents. On close scrutiny, it seems that there is a gradual decrease in  $\Phi_F$  with increasing solvent polarity but the effect is shallow and certain solvents do not follow the generic pattern. The excited-state lifetime measured in the same series of solvents decreases with increasing solvent polarity in much the same manner as found for the quantum yield. However, in polar solvents ( $\epsilon_S > 10$ ) the quality of the statistical fit to a mono-exponential decay falls below the satisfactory level.<sup>[21]</sup> This fit can be judged best in terms of the randomness of the weighted residuals,<sup>[22]</sup> but is also evident in an increased chi-squared parameter ( $\chi^2$ ) and in the Durbin-Watson term; N.B.  $\chi^2$  is given in Table 3. Inclusion of a short-lived (i.e., <1 ns) or long-lived (i.e., >10 ns) component did not improve the quality of the fit. However, analysis of the decay curves as dual-exponential fits with lifetimes in the range of 5-7 ns and 1-3 ns gave superior (i.e., more random)

residuals and  $\chi^2$  parameters closer to unity. Furthermore, the fractional contribution ( $A_1$ ) of the shorter-lived component ( $\tau_1$ ) was found to increase in significance with increasing solvent polarity (see Supporting Information). Although the two lifetimes are too close for unique solutions to be extracted from these fits, the dual-exponential behaviour appears to better represent the situation in polar solution. Even so, certain hydrogen-bond acceptor solvents, specifically N,N-diethylformamide, N,N-diethylacetamide and dimethylsulfoxide, appear to behave anomalously.

**Table 3.** Effect of solvent dielectric constant on the photophysical properties of BAB(ET) as recorded at room temperature.

| Solvent                         | $\epsilon_S$ | $\Phi_F$ | $\tau_S$ / ns <sup>[a]</sup> | $k_{RAD}$ / $10^6$ s <sup>-1</sup> | $\chi^2$ <sup>[b]</sup> |
|---------------------------------|--------------|----------|------------------------------|------------------------------------|-------------------------|
| Toluene                         | 2.43         | 0.78     | 5.74                         | 1.36                               | 0.95                    |
| Dibutyl ether                   | 3.18         | 0.83     | 6.85                         | 1.21                               | 0.92                    |
| Diethyl ether                   | 4.33         | 0.86     | 6.35                         | 1.35                               | 1.05                    |
| CHCl <sub>3</sub>               | 4.89         | 0.85     | 6.45                         | 1.32                               | 1.07                    |
| Ethyl acetate                   | 6.02         | 0.82     | 6.60                         | 1.24                               | 1.06                    |
| MTHF                            | 7.47         | 0.79     | 6.60                         | 1.20                               | 0.99                    |
| THF                             | 7.58         | 0.75     | 5.85                         | 1.28                               | 0.96                    |
| CH <sub>2</sub> Cl <sub>2</sub> | 9.02         | 0.78     | 6.17                         | 1.26                               | 1.12                    |
| Heptyl cyanide                  | 13.0         | 0.68     | 6.10                         | 1.12                               | 1.30                    |
| Valeronitrile                   | 20.0         | 0.58     | 6.00                         | 0.97                               | 1.43                    |
| Acetone                         | 21.4         | 0.67     | 6.00                         | 1.12                               | 1.12                    |
| Ethanol                         | 24.3         | 0.48     | 5.60                         | 0.86                               | 1.39                    |
| Butyronitrile                   | 24.6         | 0.55     | 5.90                         | 0.93                               | 1.52                    |
| Nitropropane                    | 27.3         | 0.46     | 5.55                         | 0.83                               | 1.87                    |
| Propionitrile                   | 28.9         | 0.44     | 5.60                         | 0.79                               | 1.51                    |
| DEF <sup>[c]</sup>              | 29.0         | 0.66     | 6.05                         | 1.09                               | 1.09                    |
| Chloroacetonitrile              | 30.0         | 0.51     | 4.85                         | 1.05                               | 1.73                    |
| Methanol                        | 33.6         | 0.43     | 4.15                         | 1.04                               | 1.87                    |
| Acetonitrile                    | 37.5         | 0.35     | 3.35                         | 1.05                               | 2.20                    |
| DEA <sup>[d]</sup>              | 38.3         | 0.66     | 5.65                         | 1.17                               | 1.32                    |
| DMSO <sup>[e]</sup>             | 46.7         | 0.64     | 5.74                         | 1.11                               | 1.28                    |

[a] Lifetime of the excited-singlet state based on a single-exponential fit. [b] Reduced chi-squared parameter associated with the single-exponential fit. [c] DEF = N,N-Diethylformamide. [d] DEA = N,N-Diethylacetamide. [e] DMSO = Dimethylsulfoxide.

At relatively low levels of precision, the dual-exponential or stretched-exponential fits give an adequate representation of the time-resolved emission decay profiles. At higher levels of precision, these fits become less satisfactory in terms of the

randomness of the residuals and it is necessary to add a third exponential term. Even so, unique solutions could not be recovered from data collected over different time scales or count rates. An additional problem is that the derived lifetimes are too similar for accurate analysis. Under such conditions, it is impossible to justify the use of two or three discrete lifetimes as opposed to a continuous distribution of lifetimes. Certainly, the molecular structure is not suggestive of several discrete conformations because of what might be considered facile rotations. This situation is not uncommon in fluorescence spectroscopy, especially with regards to biologically relevant materials, and has led to the introduction of the maximum entropy method<sup>[23]</sup> (MEM). This analytical approach, modified to increase reliability about the zero-time shift,<sup>[24]</sup> allows recovery of the shape of distributions of lifetimes. The MEM method allows determination of the coefficients of an exponential series of pre-set lifetimes isolated from correlation effects and instrumental oscillations.

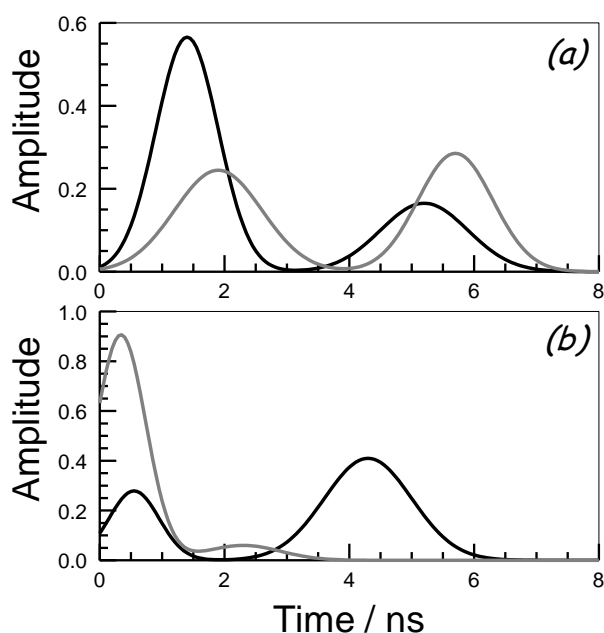


**Figure 4.** Maximum entropy method plots derived by fitting the deconvoluted emission decay curves for (a) BAB(ET) and (b) BAB(H) in butyronitrile (grey curve) and acetonitrile (black curve). See the text and Table 5 for the derived parameters.

Using a variety of time ranges for each sample, it proved possible to recover reproducible lifetime distributions for BAB(ET) in polar and weakly polar solvents. In each case, the longer-lived species gave a lifetime of around 4-6 ns while the shorter-lived component was in the region of 1-2 ns (Figure 4a). There was no obvious correlation between mean lifetime and solvent polarity but the total contribution of the shorter-lived species, integrated

as a Gaussian profile, increased progressively with increasing  $\epsilon_S$  (see Supporting Information). Thus, based on the MEM analysis, there appears to be a wide variety of slowly interconverting conformers that fall into two loose families, which differ in terms of the relative radiative probability of the BODIPY fluorophores

It might be important to stress that  $\epsilon_S$  is not the only means for expressing solvent polarity<sup>[25]</sup> and, in fact, several alternatives are available. These include Reichardt's empirical ET(30) parameter,<sup>[26]</sup> the Kirkwood factor<sup>[27]</sup> and the Catalan SPP<sup>[28]</sup> and SB<sup>[29]</sup> factors. It is not the purpose of the present investigation to critically compare these solvent descriptors but it should be emphasized that similar behavior is noted in all cases with regards to the polarity effect on fluorescence probability.

**Table 4.** Effect of solvent dielectric constant on the photophysical properties of BAB(H) as recorded at room temperature.

| Solvent                         | $\epsilon_S$ | $\Phi_F$ | $\tau_S$ / ns <sup>[a]</sup> | $k_{RAD}$ / $10^8$ s <sup>-1</sup> | $\chi^2$ <sup>[b]</sup> |
|---------------------------------|--------------|----------|------------------------------|------------------------------------|-------------------------|
| Toluene                         | 2.43         | 0.60     | 4.19                         | 1.43                               | 1.02                    |
| Dibutyl ether                   | 3.18         | 0.65     | 4.50                         | 1.44                               | 0.96                    |
| Diethyl ether                   | 4.33         | 0.71     | 5.15                         | 1.38                               | 0.97                    |
| CHCl <sub>3</sub>               | 4.89         | 0.73     | 5.52                         | 1.32                               | 1.10                    |
| Ethyl acetate                   | 6.02         | 0.74     | 5.23                         | 1.41                               | 1.08                    |
| MTHF                            | 7.47         | 0.73     | 4.88                         | 1.50                               | 1.18                    |
| THF                             | 7.58         | 0.73     | 5.36                         | 1.36                               | 1.14                    |
| CH <sub>2</sub> Cl <sub>2</sub> | 9.02         | 0.63     | 5.40                         | 1.17                               | 1.38                    |
| Heptyl cyanide                  | 13.0         | 0.66     | 5.20                         | 1.27                               | 1.53                    |
| Valeronitrile                   | 20.0         | 0.56     | 5.14                         | 1.10                               | 1.82                    |
| Acetone                         | 21.4         | 0.50     | 5.18                         | 0.97                               | 1.48                    |
| Ethanol                         | 24.3         | 0.46     | 4.60                         | 1.00                               | 1.94                    |
| Butyronitrile                   | 24.6         | 0.44     | 4.55                         | 0.97                               | 2.11                    |
| Nitropropane                    | 27.3         | 0.39     | 3.57                         | 1.11                               | 1.82                    |
| Propionitrile                   | 28.9         | 0.23     | 1.96                         | 1.12                               | 2.35                    |
| DEF <sup>[c]</sup>              | 29.0         | 0.48     | 4.85                         | 1.00                               | 1.60                    |
| Chloroacetonitrile              | 30.0         | 0.21     | 1.91                         | 1.10                               | 2.28                    |
| Methanol                        | 33.6         | 0.19     | 1.00                         | 1.90                               | 2.35                    |
| Acetonitrile                    | 37.5         | 0.07     | 0.74                         | 0.95                               | 3.10                    |
| DEA <sup>[d]</sup>              | 38.3         | 0.42     | 3.92                         | 1.07                               | 2.23                    |
| DMSO <sup>[e]</sup>             | 46.7         | 0.12     | 0.90                         | 1.33                               | 1.93                    |

[a] Lifetime for the excited-singlet state as recovered from single-exponential fits. [b] Reduced chi-squared parameter associated with the singlet-exponential fits. [c] DEF = N,N-diethylformamide. [d] DEA = N,N-diethylacetamide. [e] DMSO = dimethylsulfoxide.

An increased level of solvent sensitivity is displayed by BAB(H) across the same series of solvents (Table 4). In general, increasing  $\epsilon_S$  tends to decrease  $\Phi_F$ , although the overall behavior is non-linear and again there are a few anomalous solvents. These latter solvents are identified as being acetone ( $\epsilon_S = 21.4$ ), N,N-diethylformamide ( $\epsilon_S = 29$ ), N,N-diethyl-acetamide ( $\epsilon_S = 38.3$ ) and dimethylsulfoxide ( $\epsilon_S = 46.7$ ) and are hydrogen-bond acceptors. As such, these solvents might be expected to form a hydrogen bond with the amide proton and thereby perturb the molecular conformation. Otherwise, protic and aprotic solvents follow a common trend and there is no indication that solvent attachment to the aza-N atoms is important in the fluorescence quenching process. In mixtures of THF ( $\epsilon_S = 7.6$ ) and acetonitrile ( $\epsilon_S = 37.5$ ),  $\Phi_F$  decreases progressively with increasing mole fraction of acetonitrile while that for BOD, used as the control, shows no such effect (Figure 5).

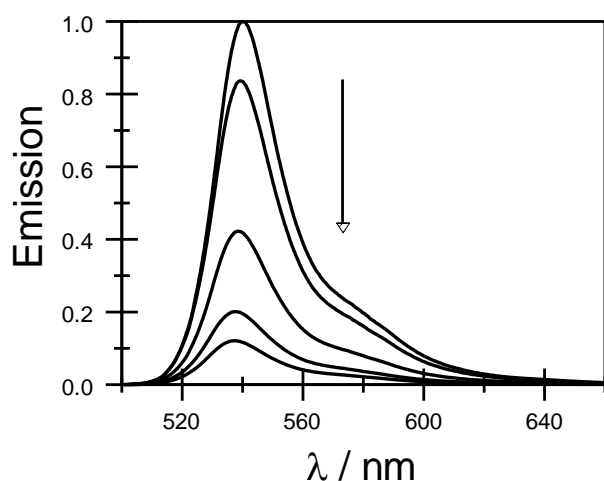


**Figure 5.** Effect of solvent composition on the fluorescence intensity recorded for BAB(H). The arrow indicates the direction of increasing mole fraction of acetonitrile in the mixture with THF; individual spectra refer to acetonitrile mole fractions of 0, 0.44, 0.61, 0.76 and 1.0.

As above, the fluorescence decay curves recorded for BAB(H) could be analyzed satisfactorily in terms of mono-exponential fits in non-polar (i.e.,  $\epsilon_S < 8$ ) solvents. However, with increasing solvent polarity the quality of the exponential fit was seen to worsen; this judgement was based<sup>[21]</sup> on the reduced chi-squared parameters ( $\chi^2$  in Table 4) and the randomness<sup>[22]</sup> of the weighted residuals. Furthermore, the radiative rate constant ( $k_{\text{RAD}} = \Phi_F/\tau_S$ ) adopts a strong dependence on solvent polarity that does not seem justified.<sup>[30]</sup> The quality of the fit improved on inclusion of a second component, corresponding to a species with a shorter lifetime, but analysis of different decay profiles recorded for the same solvent on differing time bases did not return unique lifetime values. Again, data collected at high precision required analysis in terms of three discrete lifetimes.

Using the MEM analytical approach, it was possible to realize reproducible fits to two broad distributions of lifetimes in polar and

weakly polar solvents (Figure 4b). The shorter-lived distribution had a mean lifetime of ca. 0.5 ns while the second series correspond to a mean lifetime of ca. 3 ns (Table 5). The total contribution of the shorter component increased in more polar solvents but the mean lifetime did not correlate with  $\epsilon_S$ . We are led to the conclusion that the reduced quantum yield arises from increased population of a family of bichromophores more susceptible to intramolecular fluorescence quenching. The nature of the solvent determines the extent of this population but there is no relationship between the level of quenching inherent to that family and the solvent polarity.

**Table 5.** Summary of the parameters derived from the MEM-based analysis of the time-resolved emission data collected for BAB(H) in polar solvents at room temperature.

| Solvent                         | $\epsilon_S$ | $\tau_A$ / ns <sup>[a]</sup> | $\tau_B$ / ns | $A_1$ | $\chi^2$ <sup>[b]</sup> |
|---------------------------------|--------------|------------------------------|---------------|-------|-------------------------|
| CH <sub>2</sub> Cl <sub>2</sub> | 9.02         | 1.80                         | 5.1           | 0.14  | 1.51                    |
| Heptyl cyanide                  | 13.0         | 0.84                         | 5.5           | 0.14  | 1.47                    |
| Valeronitrile                   | 20.0         | 0.30                         | 4.85          | 0.16  | 1.90                    |
| Acetone                         | 21.4         | 1.45                         | 3.9           | 0.09  | 1.15                    |
| Ethanol                         | 24.3         | 1.00                         | 3.65          | 0.10  | 1.44                    |
| Butyronitrile                   | 24.6         | 0.55                         | 4.3           | 0.28  | 1.09                    |
| Nitropropane                    | 27.3         | 0.23                         | 3.75          | 0.25  | 1.68                    |
| Propionitrile                   | 28.9         | 0.33                         | 3.65          | 0.45  | 1.47                    |
| Chloroacetonitrile              | 30.0         | 0.27                         | 2.5           | 0.48  | 1.36                    |
| Methanol                        | 33.6         | 1.10                         | 0.65          | 0.80  | 1.90                    |
| Acetonitrile                    | 37.5         | 0.34                         | 2.3           | 0.91  | 1.15                    |
| DMSO <sup>[c]</sup>             | 46.7         | 0.80                         | 2.9           | 0.95  | 1.33                    |

[a] Mean lifetime for the shorter-lived component derived from fitting the distribution to a Gaussian profile. [b] Reduced chi-squared parameter associated with fit between simulated and experimental decay curves. [c] DMSO = dimethylsulfoxide.

## Fluorescence quenching

In consideration of the fluorescence quenching mechanism, we draw attention to the similar qualitative behavior of the two compounds but note that fluorescence quenching is much more pronounced for BAB(H) than for BAB(ET). The two bichromophores exhibit comparable optical spectroscopy and electrochemistry such that the disparate quenching level displayed in any given solvent cannot be ascribed to thermodynamic effects. The only chemical difference between the compounds relates to the substitution pattern around the amide linker. This latter group is not in electronic communication with the excited state localized on the BODIPY chromophore, suggesting that its role in the quenching event is to perturb the molecular conformation. We can also eliminate light-induced charge transfer

## FULL PAPER

between BODIPY and 1,10-phenanthroline as playing an important role since such processes are thermodynamically unfavorable, unless the latter unit is protonated. Consideration of the cyclic voltammograms and taking due allowance for the excitation energy of the BODIPY chromophore, as derived from the intersection of normalized absorption and fluorescence spectra, indicates that light-induced charge transfer between the two BODIPY units is weakly exergonic in  $\text{CH}_2\text{Cl}_2$  solution. Indeed, the thermodynamic driving force ( $-\Delta G_{\text{CS}}$ ) is 50 meV in the absence of electrostatic effects. This mechanism remains the most likely cause of the observed emission quenching in the target bichromophores and it is well established<sup>[31]</sup> that the thermodynamics for light-induced charge transfer are sensitive to the nature of the solvent. It might be mentioned that other molecules containing two BODIPY-based chromophores have reported excimer emission,<sup>[32]</sup> dimerization<sup>[33]</sup> and light-induced charge transfer<sup>[34]</sup> in fluid solution.

Based on existing theoretical principles,<sup>[31,35,36]</sup> the effects of changes in solvent polarity and mutual separation distance between the reactants on  $\Delta G_{\text{CS}}$  were simulated. The results are compiled in the Supporting Information in terms of driving force, solvent re-organization energy and overall activation energy. At any given separation distance,  $\Delta G_{\text{CS}}$  decreases sharply with increasing  $\epsilon_{\text{S}}$  but the general effect tends to saturate at high dielectric constant (i.e.,  $\epsilon_{\text{S}} > 10$ ). Similarly, at a given  $\epsilon_{\text{S}}$ ,  $\Delta G_{\text{CS}}$  decreases with decreasing separation distance but tends towards a plateau as  $R_{\text{CC}}$  exceeds ca. 10 Å. Similar effects are found for the activation energy, which requires knowledge of the re-organization energy. Most of the change is expected to occur for weakly polar solvents at quite short separations.<sup>[36,37]</sup> Although charge-transfer quenching will become more significant in polar solvents, the calculated changes in thermodynamic effects cannot explain the solvent-induced variations in fluorescence seen for these bichromophores. There are no differences in  $\Delta G_{\text{CS}}$  between BAB(ET) and BAB(H) but the level of fluorescence quenching is quite disparate. Taking into account the MEM-derived results, we can conclude that there must be an accompanying solvent-induced structural change<sup>[38]</sup> and we now examine this possibility using molecular modelling.

### Computational studies made with BAB(ET)

Molecular modelling studies (DFT, B3LPY, 6-31G(d,p)) were made with a view to better understand the mechanism of light-induced electron transfer in the two bichromophores. Starting firstly with BAB(ET), model calculations indicate that the carbonyl groups are hindered from adopting a planar orientation with the 1,10-phenanthroline unit because of steric crowding. Instead, the lowest-energy configuration has the two carbonyl groups sitting almost perpendicular to the plane of the 1,10-phenanthroline nucleus. This gives rise to two interconvertible species; namely, the opposite structure having oxygen atoms pointing away from each other and the adjacent structure having the oxygen atoms pointing in the same direction (Chart 2). For structures generated *in vacuo*, each amide group adopts the *cis*-geometry, with the opposite form providing the more stable species. The same

situation holds for structures calculated in a solvent reservoir of  $\epsilon_{\text{S}} = 20$ . However, in weakly polar solvent, there is increased likelihood that one of the carbonyl groups adopts the *trans*-geometry. In water, the lowest-energy conformation has both carbonyl groups existing as the *trans*-species, although the mixed *trans/cis* geometry is only marginally less stable in polar media. This matrix of computed structures is illustrated by way of Chart 2 and it might be stressed that it is not possible to generate a reasonable geometry for the hypothetical *cis/cis* species in the adjacent form because of severe steric crowding.

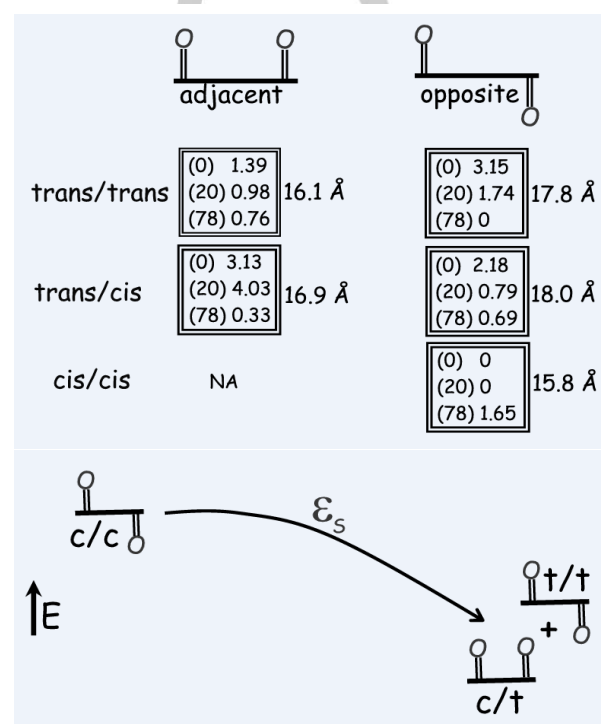


**Chart 2.** Effect of solvent polarity on the computed energies for the various conformers predicted for BAB(ET). The upper panel shows energies in kcal/mol and B-B separation distances for opposite and adjacent species; the values given in parenthesis are the solvent dielectric constants. The lower panel shows the anticipated structural evolution as the dielectric constant increases.

Calculations made for  $\epsilon_{\text{S}} = 20$  suggest the presence of several barriers for rotation of the carbonyl unit around the plane of the 1,10-phenanthroline residue. Thus, starting from the adjacent *trans/trans* geometry and rotating a single carbonyl group, the first barrier to be encountered relates to the ethyl group moving into space occupied by the *meso*-phenyl ring of the second BODIPY unit. This barrier is slightly less than 20 kcal/mol but can be reduced by concerted motion of the opposing phenyl ring. A more substantial barrier is raised by close approach of the ethyl- $\text{CH}_2$  group to the 3-H atom of the aza-aromatic unit, followed by a less severe clash between the ethyl- $\text{CH}_3$  group and the same proton. These latter barriers are essentially insurmountable at ambient temperature and restrict the direction through which the

carbonyl group can oscillate between opposite and adjacent sites (Figure 6a).

For the mixed *cis/trans* species, the carbonyl groups show only a minor preference for the opposite configuration, the difference in energy between opposite and adjacent species being only a few kcal/mol at  $\epsilon_S = 20$ . Full rotation around the *cis*-amide is not possible because of severe steric clashes. The energy-minimized geometry has the carbonyl group on the *cis*-amide lying  $85^\circ$  to the plane of the 1,10-phenanthroline residue. Rotation in one direction causes the BODIPY unit to fold back onto the 1,10-phenanthroline nucleus while rotation in the other direction brings the phenyl ring on the *cis*-amide into contact with the 1,10-phenanthroline H3 atom (Figure 6b). With the carbonyl groups in the adjacent configuration, rotation brings the BODIPY unit into contact with the ethyl group on the other amide. Interconversion between the opposite and adjacent configurations is possible only with concerted movement of the other BODIPY-based arm.

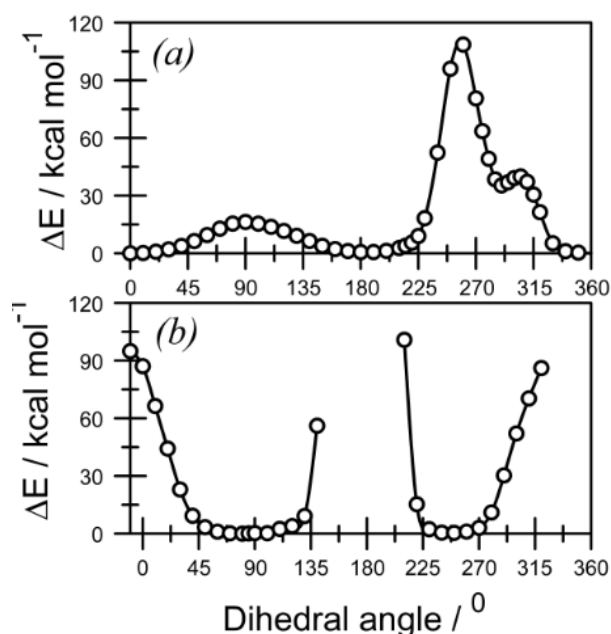


**Figure 6.** Rotational barriers computed for progressive twisting of one of the carbonyl groups present in BAB(ET) in a solvent reservoir with dielectric constant equal to 20. Panel (a) refers to the all-*trans* form with zero degrees representing the opposite form. Panel (b) refers to the *cis-trans* species with rotation around the *cis*-amide. Here, the energy-minimized geometry corresponds to a dihedral angle of  $80^\circ$ .

Similar calculations were performed for isomerisation of the amide group, starting with the *trans/trans* species with the adjacent configuration. Allowing rotation in one direction, an energy profile for isomerisation around the C-N bond<sup>[39]</sup> shows the maximum barrier of ca. 20 kcal/mol occurring at  $90^\circ$ , as might be expected.<sup>[40]</sup> As the solvent polarity increases, the barrier height is raised<sup>[41]</sup> for *trans*-to-*cis* isomerisation but decreases for the reverse step by a few kcal/mol for  $\epsilon_S = 40$ . Rotation in the opposite direction imposes an insurmountable barrier, in excess of 100

kcal/mol, which arises from steric clashes between the two BODIPY units (Figure 7). The corresponding *cis*-isomer cannot be reached by this route. A similar barrier was observed for isomerisation from the opposite configuration, although here the *cis*-isomer is the more favored product in moderately polar solvents.

Molecular dynamics simulations made for the all-*trans* tautomer in a bath of water molecules ( $50 \times 50 \times 50 \text{ \AA}^3$ )<sup>[42]</sup> using the AMBER-03 force field<sup>[43]</sup> indicate that the main structural motions relate to fluctuation of the carbonyl group around its connection to the 1,10-phenanthroline nucleus. At 250K, there is no suggestion for isomerisation of the amide bond on the time scale of the simulations. Likewise, the carbonyl group does not alternate between adjacent and opposite configurations. The all-*cis* species oscillates around the mean geometry without switching to the *trans*-form, at least on short simulations. As such, the two BODIPY units sample many different mutual orientations but remain at crude B-B separations of ca. 14-20 Å, regardless of starting geometry. None of these migratory pathways brings the BODIPY units into direct contact.

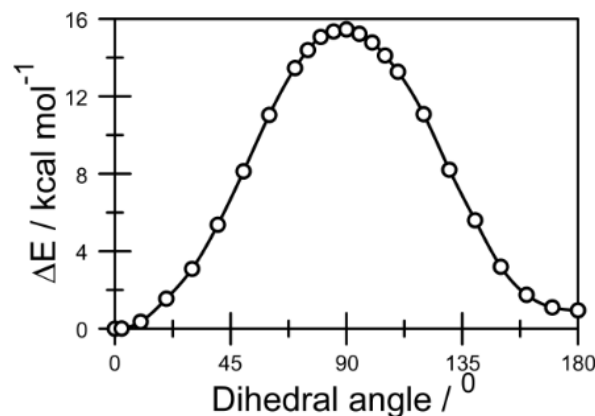


**Figure 7.** Rotational barrier computed for isomerization of an amide group for BAB(ET) in a solvent reservoir with dielectric constant equal to 20. Zero degrees corresponds to the *cis*-geometry.

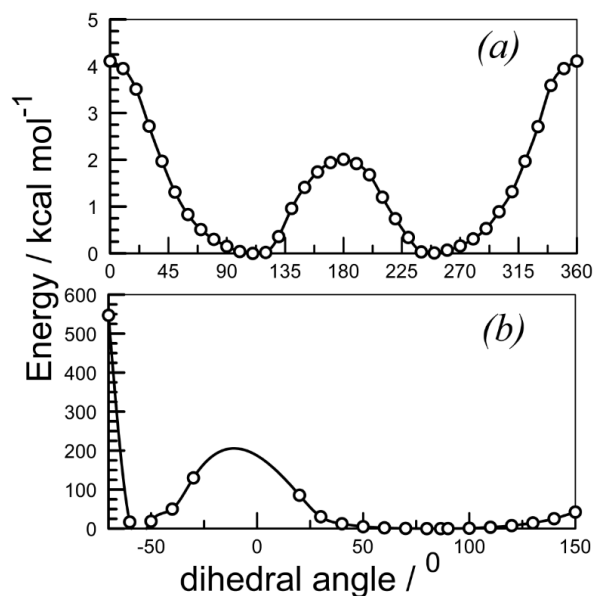
### Computational studies made with BAB(H)

Attention now turns to the bichromophore built around primary amide linkages. In order to avoid repulsion between lone pairs localized on O and aza-N atoms, the preferred dihedral angle for the carbonyl group and the heterocycle is ca.  $90^\circ$ . This configuration might be stabilized by hydrogen bonding between the carbonyl O atom and an ortho-phenyl-H atom.<sup>[44]</sup> Again, there exists the possibility for opposite and adjacent forms but these possess similar heats of formation and give rise to comparable distances between the appended BODIPY residues. The energy-minimized geometry has the amide bond in the *trans*-configuration<sup>[45]</sup> for all solvent polarities. However, the energy difference between the all-*trans* and *cis/trans* species becomes negligible at high dielectric constant. As such, in highly polar

## FULL PAPER

solvents we would expect to attain almost equal populations of the all-*trans* and *cis/trans* species.

**Figure 8.** Rotational barriers calculation for motion of the carbonyl group around



the 1,10-phenanthroline nucleus for (a) the all-*trans* and (b) all-*cis* geometries.

An energy profile<sup>[46]</sup> for rotation of the carbonyl group around the connection with the 1,10-phenanthroline nucleus, while retaining the *trans*-geometry, shows a modest barrier due to repulsion between the lone-pairs on carbonyl group and aza-N atom. The height of this barrier decreases in polar solvents and amounts to ca. 4 kcal/mol for  $\epsilon_S = 20$ . Clearly, this dihedral angle will cover a wide variance under ambient conditions. There are small differences in the calculated energies of the adjacent and opposite configurations, with increased solvent polarity moving the equilibrium position in favor of the former. This has a small effect on the average distance between the two BODIPY residues, but these units remain well separated in all cases for the *trans*-geometry.

The corresponding *cis*-amide<sup>[47]</sup> in the mixed *cis/trans* species positions the carbonyl group orthogonal to the heterocycle. Rotation in one direction is blocked by steric clashes between the two BODIPY residues. In the other direction, rotation is blocked by clashes between the phenyl ring and the 1,10-phenanthroline H3 atom. As such, the *cis*-species has the propensity to being the two BODIPY units into unusually close proximity.

The barrier for isomerisation of the amide bond is calculated<sup>[48]</sup> to be ca. 15 kcal/mol for  $\epsilon_S = 20$  but steric crowding between the two BODIPY residues prevents formation of the all-*cis* species. Calculations made for BAB(H) *in vacuo* give a barrier for isomerisation of ca. 32 kcal/mol but this falls to slightly less than 15 kcal/mol in polar solvent. In fact, the barrier height<sup>[49]</sup> becomes almost independent of solvent polarity for  $\epsilon_S > 10$ . We might expect that isomerisation will be too slow to be competitive

with decay of the excited-singlet state but can take place for the ground state. Furthermore, in non-polar solvent, the all-*trans* species will dominate but a mixture of all-*trans* and *cis/trans* species should abound in solvents of higher polarity. The *trans*-species can sample a wide variety of configurations via rotation of the carbonyl group but the *cis*-species experiences more restricted rotation. This situation seems to be in good accord with the MEM analysis in terms of there being two distinct groups of conformers.<sup>[50]</sup>

### Relationship between fluorescence quenching and molecular structure

We raise the hypothesis that the only viable mechanism able to account for the observed solvent effect on the emission properties of the BODIPY unit in these bichromophores is light-induced charge transfer<sup>[31,34,51]</sup> between the terminal dyes. As such, it is instructive to enquire if the proposed changes in molecular conformation can explain the experimental observations. For BAB(ET), the two BODIPY units are held apart under all reasonable conditions to such an extent that through-space charge transfer<sup>[52]</sup> is unlikely to compete effectively with the inherent radiative and nonradiative decay routes. Fluorescence quenching is ineffectual for this compound, except in strongly polar media. Polar solvent promotes conversion of the *cis*-species to the corresponding *trans*-tautomer. Our modelling studies would suggest that, in strongly polar media, the bichromophore should persist as a mixture of all-*trans* and *cis/trans* isomers. Combining this result with the fluorescence behavior, we can speculate that the *trans*-geometry provides a better conduit<sup>[53]</sup> for through-bond charge transfer. The long pathway so involved,<sup>[54]</sup> together with the modest thermodynamic driving force, means emission quenching will be kept at a minimum, as is observed. The mean difference between the two sets of emission lifetimes, taken together with the lifetime of the control compound, translates to a ratio of rate constants for charge-separation of 2-fold in favor of the *trans*-amide.

There is, in fact, ample evidence to indicate that the *trans* geometry provides a better pathway for super-exchange interactions in many different types of molecular bridge.<sup>[55-58]</sup> This is attributed to improved electronic coupling and nicely explains the observations made with BAB(ET). The computational studies suggest that the all-*cis* species will predominate in non-polar solvents and also in weakly polar media. Strongly polar solvents, however, trigger the switch to the *trans*-geometry and we would expect to see increased population of the *trans/cis* species in the more polar solvents. Isomerisation is unlikely to be competitive with inherent deactivation of the excited-state. Instead, illumination of the ground-state equilibrium will produce a distribution of geometries that do not interconvert on the existing time scale. This situation would equate to two families of conformers, each displaying a range of nonradiative rate constants representing the mean geometry at the moment of excitation. In turn, this would lead to the type of distributed lifetimes consistent with the MEM analysis.

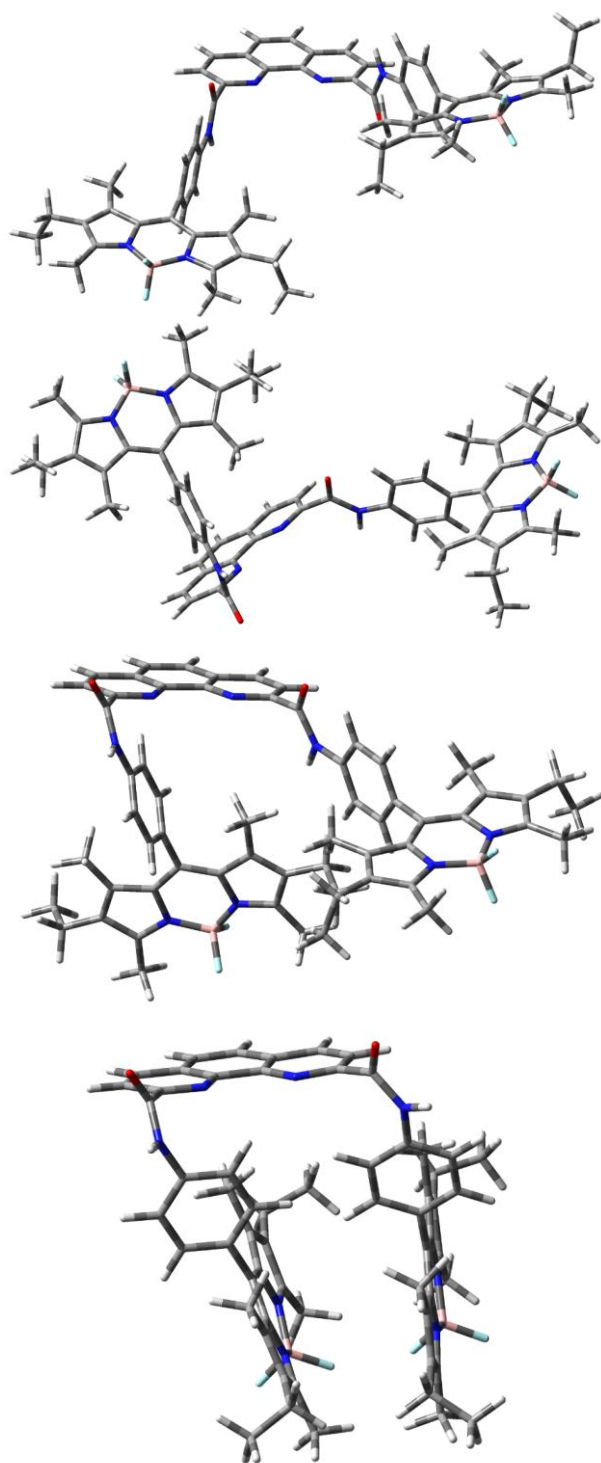


**Figure 9.** Snapshots of molecular conformations representing the important distributions for all-*trans* (uppermost panel), mixed-*cis/trans* (central panels), and all-*cis* (lower panel) geometries for BAB(H) in solution.

Quite unexpectedly, there are major structural differences between BAB(ET) and BAB(H) caused by internal steric crowding and/or electronic effects. Fluorescence quenching becomes more significant for BAB(H), although the thermodynamic driving force is the same as that for BAB(ET) and there is a similar sensitivity towards solvent polarity. Calculations made for BAB(H) predict that the *trans* geometry is favored in all solvents, this being the opposite situation to that found for BAB(ET), but polar solvent promotes transformation to the *cis* isomer. In non-polar solvents, we would expect to see only the all-*trans* species. Increasing the solvent polarity raises the possibility for finding *trans/cis* species.

By analogy to BAB(ET), increasing the contribution of the *cis*-species might be expected to extinguish through-bond charge separation. This would restore fluorescence. However, for BAB(H) the *cis/trans* species has the two BODIPY units close together, contact being possible in the extreme case, while rotation around one of the carbonyl groups further reduces the edge-to-edge separation (Figure 9). As such, the *cis*-isomer can be expected to promote through-space, light-induced charge separation<sup>[57]</sup> between the two BODIPY units. This situation would introduce a short-lived component into the decay records in polar solvents. Since each isomer samples a variety of conformations, the lifetime distributions provided by the MEM analysis appear to mirror the solvent-induced conformational change.

It might be noted that transient absorption spectral studies did not indicate the formation of an intermediate species with a lifetime longer than that of the excited-singlet state. Thus, laser excitation of BAB(ET) in deaerated CH<sub>3</sub>CN solution at 400 nm indicated the presence of the S<sub>1</sub> state immediately after the pulse. This species is recognized by strong bleaching the lowest-energy absorption transition centred at around 525 nm, together with weak absorption bands at higher and lower energy. There is an accompanying contribution from stimulated fluorescence. The signal decays with an approximate lifetime of 3.0 ± 0.7 ns to restore the pre-pulse baseline. Although the decay kinetics are not strictly mono-exponential, global analysis of the transient spectra recorded at different time delays showed only the S<sub>1</sub> state to be present. The same conclusion was reached for BAB(H) in CH<sub>3</sub>CN, where the recovery of the transient bleaching signal at 525 nm could be analysed as the sum of two exponential terms, with lifetimes of 0.4 ± 0.1 (80%) and 2.1 ± 0.5 (20%) ns. Again, no transient species could be observed. This behavior is not unusual and indicates that subsequent charge recombination occurs on a faster time scale than does light-induced charge transfer.<sup>[59]</sup> The former process will be assisted by electrostatic attractive forces that should minimize separation between the two BODIPY units.

## Conclusions

This work has shown that the amide linkage provides for multiple molecular conformations that differ in terms of their propensity to promote either through-bond or through-space charge transfer. In addition to isomerisation around the central C-N amide bond, structural complications arise from electronic interactions between the carbonyl O atom and the aza-N atom of the 1,10-phenanthroline unit. Indeed, the BODIPY-based arms attached to

the heterocyclic linker provide a crude cavity wherein hydrogen-bonding and steric interactions further restrict conformational freedom to such an extent that the two target compounds appear structurally distinct. This situation is exemplified by the realization that BAB(ET) adopts the *cis*-geometry while BAB(H) takes up the *trans*-geometry. These various conformations influence the quantum yield for fluorescence from the BODIPY appendages, but quenching is kept to a minimum by limited thermodynamics. It seems likely that these effects could be greatly amplified by appropriate choice of the terminals. Thus, the amide linkage might offer some unusual opportunities to switch between emissive and dark states under suitable stimulation. This situation is made possible because the absolute energies of the various tautomers are quite comparable while rotational barriers will impose kinetic limitations at the excited-state level.

## Experimental Section

Experimental details for the synthesis of the target compounds are provided as part of the Supporting Information. Solvents used for the spectroscopic studies were obtained from commercial sources and were checked for fluorescent impurities before use. Absorption spectra were recorded with a Hitachi U-3310 spectrophotometer while emission spectra were recorded with a Hitachi F-4500 spectrophotometer. Fluorescence spectra were recorded for optically dilute solution, the absorbance being less than 0.1 at the excitation wavelength, and were fully corrected for any instrumental imperfections. Fluorescence quantum yields were recorded relative to monomeric BODIPY derivatives already reported in the literature. Emission lifetimes were recorded via time-correlated, single photon counting methodologies using a short duration laser diode emitting at 505 nm for excitation. Quantum chemical calculations were made with TURBOMOLE and are described in more detail in the Supporting Information.

## Acknowledgements

We thank Newcastle University, BRNS (BARC), and ECPM-Strasbourg for their financial support of this work. Dr. J. G. Knight (Newcastle University) is acknowledged for many helpful discussions on the chemistry of the amide bond.

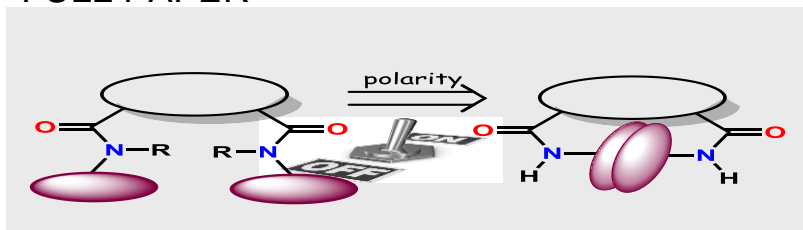
**Keywords:** conformational exchange • isomerization • fluorescence • charge transfer • BODIPY dyes

- [1] D. Whitford, *Proteins: Structure and Function*, John Wiley & Sons, Chichester, 2005 (ISBN 0-471-49893-9).
- [2] N. Seward, H.-D. Jakubke, *Peptides: Chemistry and Biology*, Wiley-VCH, 2<sup>nd</sup> Edition, Weinheim, 2009 (ISBN 978-3-527-31867-4).
- [3] E. Iglesias, L. Montenegro, *J. Chem. Soc., Faraday Trans.* **1996**, *92*, 1205-1212.
- [4] a) D. B. Brown, M. B. Robin, R. D. Burbank, *J. Am. Chem. Soc.* **1968**, *90*, 5621-5622; b) D. P. Fairlie, T. C. Woon, W. A. Wickramasinghe, A. C. Willis, *Inorg. Chem.* **1994**, *33*, 6425-6428; c) C. R. Kemnitz, M. J. Loewen, *J. Am. Chem. Soc.* **2007**, *129*, 2521-2528; d) E. M. Duffy, D. L. Severance, W. L. Jorgensen, *J. Am. Chem. Soc.* **1992**, *114*, 7535-7542; e) J. Zhang, M. W. Germann, *Biopolym.* **2011**, *95*, 755-762.
- [5] (a) H. B. Schlegel, P. Gund, E. M. Fluder, *J. Am. Chem. Soc.*, **1982**, *104*, 5347-5351. (b) K. B. Wiberg, P. R. Rablen, D. J. Rush, T. A. Keith, *J. Am. Chem. Soc.* **1995**, *117*, 4261-4270.
- [6] K. Kamiya, M. Boero, K. Shiraiishi, A. Oshiyama, *J. Phys. Chem.* **B2006**, *110*, 4443-4450.
- [7] P. I. Nagy, *Biochem. Pharmacol.* **2013**, *S4*, 1-23.
- [8] P. J. Cragg, *Supramolecular Chemistry: From Biological Inspiration to Biomedical Applications*, Springer, Dordrecht, 2010 (ISBN 978-90-481-2581-4).
- [9] a) A. Loudet, K. Burgess, *Chem. Rev.* **2007**, *107*, 4891-4932; b) G. Ulrich, R. Ziessel, A. Harriman, *Angew. Chem. Int. Ed.* **2008**, *47*, 1184-1201; c) N. Boens, V. Leen, W. Dehaen, *Chem. Soc. Rev.* **2012**, *41*, 1130-1172; d) A. Kamkaew, S. H. Lim, H. B. Lee, L. V. Kiew, L. Y. Chung, K. Burgess, *Chem. Soc. Rev.* **2013**, *42*, 77-88; e) H. Lu, J. Mack, Y. Yanga, Z. Shen, *Chem. Soc. Rev.* **2014**, *43*, 4778-4823.
- [10] a) M. A. H. Alamiry, E. Bahaidarah, A. Harriman, J. H. Olivier, R. Ziessel, *Pure Appl. Chem.* **2013**, *85*, 1349-1365; b) A. Harriman, R. Ziessel, *Photochem. Photobiol. Sci.* **2010**, *9*, 960-967.
- [11] a) R. Ziessel, G. Ulrich, A. Harriman, *New J. Chem.* **2007**, *31*, 496-501; b) A. C. Benniston, G. Copley, *Phys. Chem. Chem. Phys.* **2009**, *11*, 4124-4130; c) M. Gupta, S. Mula, M. Tyagi, T. K. Ghanty, S. Murudkar, A. K. Ray, S. Chattopadhyay, *Chem. Eur. J.* **2013**, *19*, 17766-17772.
- [12] J. Rosenthal, A. B. Nepomnyashchii, J. Kozhukh, A. J. Bard, S. J. Lippard, *J. Phys. Chem. C* **2011**, *115*, 17993-18001.
- [13] V. Munoz, L. Serrano, *Nature Struc. Biol.* **1994**, *1*, 399-409.
- [14] A. Ben-Naim, *Adv. Biol. Chem.* **2013**, *3*, 29-39 and references cited therein.
- [15] a) S. Mula, G. Ulrich, R. Ziessel, *Tetrahedron Lett.* **2009**, *50*, 6383-6388; b) S. Mula, K. Elliott, A. Harriman, R. Ziessel, *J. Phys. Chem. A* **2010**, *114*, 10515-10522.
- [16] a) H. Sajiki, T. Ikawa, K. Hirota, *Org. Lett.* **2004**, *6*, 4977-4980; b) R. Nakarño, S. Kotakonda, D. M. D. Fouchard, L. M. V. Tillekeratne, R. A. Hudson, *Org. Lett.* **2005**, *7*, 471-474.
- [17] a) C. J. Chandler, L. W. Deady, J. A. Reiss, *J. Heterocycl. Chem.* **1981**, *18*, 599-601; b) D. Manna, S. Mula, A. Bhattacharyya, S. Chattopadhyay, T. K. Ghanty, *Dalton Trans.* **2015**, *44*, 1332-1340.
- [18] a) R. Ziessel, L. Bonardi, P. Retailleau, G. Ulrich, *J. Org. Chem.* **2006**, *71*, 3093-3102; b) T. Bura, R. Ziessel, *Tetrahedron Lett.* **2010**, *51*, 2875-2879; c) N. Shivran, S. Mula, T. K. Ghanty, S. Chattopadhyay, *Org. Lett.* **2011**, *13*, 5870-5873.
- [19] a) J. Karolin, L. B. A. Johansson, L. Strandberg, T. Ny, *J. Am. Chem. Soc.* **1994**, *116*, 7801-7806; b) A. Burghart, H. J. Kim, M. B. Welch, L. H. Thorensen, J. Reibenspies, K. Burgess, F. Bergstrom, L. B. A. Johansson, *J. Org. Chem.* **1999**, *64*, 7813-7819; c) H. Sunahara, Y. Urano, H. Kojima, T. Nagano, *J. Am. Chem. Soc.* **2007**, *129*, 5597-5604; d) K. K. Jagtap, N. Shivran, S. Mula, D. B. Naik, S. K. Sarkar, T. Mukherjee, D. K. Maity, A. K. Ray, *Chem. Eur. J.* **2013**, *19*, 702-708.
- [20] W. W. Qin, M. Baruah, M. Van der Auweraer, F. C. De Schryver, *J. Phys. Chem. A* **2005**, *109*, 7371-7384.
- [21] D. V. O'Connor, D. Phillips, *Time-Correlated Single Photon Counting*, Academic Press, New York, 1979.
- [22] K. Santa, J. C. Zhan, X.-Y. Song, E. A. Smith, N. Vaswani, J. W. Petrich, *J. Phys. Chem. B* **2016**, *120*, 2484-2490.
- [23] A. Siemiarz, B. D. Wagner, W. R. Ware, *J. Phys. Chem.* **1990**, *94*, 1661-1666.
- [24] R. Esposito, G. Mensitieri, S. de Nicola, *Analyst* **2015**, *140*, 8138-8147.
- [25] A. R. Katritzky, D. C. Fara, H. Yang, K. Tamm, T. Tamm, M. Karelson, *Chem. Rev.* **2004**, *104*, 175-198.
- [26] C. Reichardt, *Chem. Rev.* **1994**, *94*, 2319-2358.
- [27] Y. Q. Zhou, G. Stell, *J. Chem. Phys.* **1992**, *96*, 1507-1515.
- [28] J. Catalán, V. López, P. Pérez, R. Martín-Villamil, J.-G. Rodríguez, *Liebigs Ann.* **1995**, 241-252.
- [29] J. Catalán, C. Diaz, V. López, P. Pérez, J. L. G. De Paz, J.-G. Rodríguez, *Liebigs Ann.* **1996**, 1785-1794.
- [30] S. J. Strickler, R. A. Berg, *J. Chem. Phys.* **1962**, *37*, 814-822.

- [31] a) M. R. Wasielewski, *Chem. Rev.* **1992**, *92*, 435-461; b) R. Ziessel, B. D. Allen, D. B. Rewinska, A. Harriman, *Chem. Eur. J.* **2009**, *15*, 7382-7393.
- [32] a) M. A. H. Alamiry, A. C. Benniston, G. Copley, A. Harriman, D. Howgego, *J. Phys. Chem. A* **2011**, *115*, 12111-12119; b) N. Saka, T. Dinc, E. U. Akkaya, *Tetrahedron* **2006**, *62*, 2721-2725; c) H. L. Qi, J. J. Teesdale, R. C. Pupillo, J. Rosenthal, A. J. Bard, *J. Am. Chem. Soc.* **2013**, *135*, 13558-13566.
- [33] a) A. Harriman, L. J. Mallon, B. Stewart, G. Ulrich, R. Ziessel, *Eur. J. Org. Chem.* **2007**, 3191-3198; b) A. N. Kursunlu, *Tetrahedron Lett.* **2015**, *56*, 1873-1877; c) R. Misra, B. Dhokale, T. Jadhav, S. M. Mobin, *New J. Chem.* **2014**, *38*, 3579-3585; d) S. Choi, J. Bouffard, Y. Kim, *Chem. Sci.* **2014**, *5*, 751-755; e) A. B. Nepomnyashchii, M. Broring, J. Ahrens, A. J. Bard, *J. Am. Chem. Soc.* **2011**, *133*, 8633-8645.
- [34] a) M. T. Whited, N. M. Patel, S. T. Roberts, K. Allen, P. I. Djurovich, S. E. Bradforth, M. E. Thompson, *Chem. Commun.* **2012**, *48*, 284-286; b) A. C. Benniston, G. Copley, A. Harriman, D. Howgego, R. W. Harrington, W. Clegg, *J. Org. Chem.* **2010**, *75*, 2018-2027.
- [35] P. F. Barbara, T. J. Meyer, M. A. Ratner, *J. Phys. Chem.* **1996**, *100*, 13148-13168.
- [36] a) D. Rehm, A. H. Weller, *Isr. J. Chem.* **1970**, *8*, 259-271; b) D. Rehm, A. H. Weller, *Ber. Bunsen-Ges. Phys. Chem.* **1969**, *73*, 834-839; c) D. Rehm, A. H. Weller, *Z. Phys. Chem. NF* **1982**, *133*, 93-98.
- [37] G. King, A. Warshel, *J. Chem. Phys.* **1990**, *93*, 8682-8692.
- [38] T. Otsu, K. Ishii, T. Tahara, *Nature Commun.* **2015**, *6*, 7685.
- [39] A. G. Martinez, E. T. Vilar, A. G. Fraile, P. Martinez-Ruiz, *J. Phys. Chem. A* **2002**, *106*, 4942-4950.
- [40] S. Samdal, *J. Mol. Struct.* **1998**, *440*, 165-174.
- [41] Y. A. Mantz, H. Gerard, R. Iftimie, G. J. Martyna, *J. Phys. Chem. B* **2006**, *110*, 13523-13538.
- [42] V. Lounnas, S. K. Ludemann, R. C. Wade, *Biophys. Chem.* **1999**, *78*, 157-182.
- [43] C. G. Ricci, A. S. de Andrade, M. Mottin, P. A. Netz, *J. Phys. Chem. B* **2010**, *114*, 9882-9893.
- [44] D. A. Dixon, K. D. Dobbs, J. J. Valenti, *J. Phys. Chem.* **1994**, *98*, 13435-13439.
- [45] E. Beausoleil, W. D. Lubell, *J. Am. Chem. Soc.* **1996**, *118*, 12902-12908.
- [46] M. A. Leiva, R. G. E. Morales, V. Vargas, *J. Phys. Org. Chem.* **1996**, *9*, 455-458.
- [47] G. Fischer, *Chem. Soc. Rev.* **2000**, *29*, 119-127.
- [48] Y. K. Yang, H. S. Park, *J. Mol. Struct. THEOCHEM* **2004**, *676*, 171-176.
- [49] A. Radzicka, L. Pedersen, R. Wolfenden, *Biochem.* **1988**, *27*, 4538-4541.
- [50] F. B. Dias, M. Knaapila, A. P. Monkman and H. D. Burrows, *Macromol.* **2006**, *39*, 1598-1606.
- [51] J. M. Giamo, A. V. Gusev, M. R. Wasielewski, *J. Am. Chem. Soc.* **2002**, *124*, 8530-8532.
- [52] V. Bandi, H. B. Gobeze, P. A. Karr, F. D'Souza, *J. Phys. Chem. C* **2014**, *118*, 18969-18982.
- [53] (a) R. M. Williams, *Photochem. Photobiol. Sci.* **2010**, *9*, 1018-1026. (b) B. P. Paulson, L. A. Curtiss, B. Bal, G. L. Closs, J. R. Miller, *J. Am. Chem. Soc.* **1996**, *118*, 378-387. (c) A. M. Oliver, D. C. Craig, M. N. Paddon-Row, J. Kroon, J. W. Verhoeven, *Chem. Phys. Lett.* **1988**, *150*, 366-373.
- [54] A. M. Brun, A. Harriman, V. Heitz, J.-P. Sauvage, *J. Am. Chem. Soc.* **1991**, *113*, 8657-8663.
- [55] A. C. Benniston, A. Harriman, *Chem. Soc. Rev.* **2006**, *35*, 169-179.
- [56] M. N. Paddon-Row, *Aust. J. Chem.* **2003**, *56*, 729-748.
- [57] K. Pettersson, J. Wiberg, T. Ljungdahl, J. Martensson, B. Albinsson, *J. Phys. Chem. A* **2006**, *110*, 319-326.
- [58] A. Harriman, V. Heitz, J.-P. Sauvage, *J. Phys. Chem.* **1993**, *97*, 5940-5946.
- [59] a) K. J. Elliott, A. Harriman, L. Le Pleux, Y. Pellegrin, E. Blart, C. R. Mayer, F. Odobel, *Phys. Chem. Chem. Phys.* **2009**, *11*, 8767-8773; b) A. Harriman, K. J. Elliott, M. A. H. Alamiry, L. Le Pleux, M. Severac, Y. Pellegrin, E. Blart, C. Fosse, C. Cannizzo, C. R. Mayer, F. Odobel, *J. Phys. Chem. C* **2009**, *113*, 5834-5842.

## Entry for the Table of Contents

## FULL PAPER



Polar solvent triggers a conformational change from *cis*- to *trans*-geometries for a tertiary amide-bridged molecular dyad but the exact opposite situation is found for the corresponding secondary amide-bridged bichromophore.

Shrikant Thakare, Patrycja Stachelek,  
Soumyaditya Mula, Ankush B. More,  
Subrata Chattopadhyay, Alok K. Ray,  
Nagaiyan Sekar, Raymond Ziessel\* and  
Anthony Harriman†

Page No. – Page No.

**Solvent-Driven Conformational  
Exchange for Amide-Linked  
Bichromophoric BODIPY Derivatives**